Arachidonate 12-lipoxygenase and 12-hydroxyeicosatetraenoic acid contribute to stromal aging-induced progression of pancreatic cancer

Received for publication, January 25, 2020, and in revised form, April 2, 2020 Published, Papers in Press, April 7, 2020, DOI 10.1074/jbc.RA120.012798

Ehab H. Sarsour[‡], Jyung Mean Son[§], Amanda L. Kalen[¶], Wusheng Xiao[‖], Juan Du[**], Matthew S. Alexander[**], Brianne R. O'Leary[**], Joseph J. Cullen[**], and Prabhat C. Goswami[¶1]

*From the [‡]Department of Basic Sciences, College of Osteopathic Medicine, Kansas City University of Medicine and Biosciences, Kansas City, Missouri 90089, the [§]Leonard Davis School of Gerontology, University of Southern California, Los Angeles, California 64106, the Departments of [¶]Radiation Oncology and **Surgery, The University of Iowa, Iowa City, Iowa 52242, and the [‖]Division of Cardiovascular Medicine, Department of Medicine, Brigham and Women's Hospital and Harvard Medical School, Boston, Massachusetts 02115*

Edited by Ruma Banerjee

The incidence of pancreatic cancer increases with age, suggesting that chronological aging is a significant risk factor for this disease. Fibroblasts are the major nonmalignant cell type in the stroma of human pancreatic ductal adenocarcinoma (PDAC). In this study, we investigated whether the chronological aging of normal human fibroblasts (NHFs), a previously underappreciated area in pancreatic cancer research, influences the progression and therapeutic outcomes of PDAC. Results from experiments with murine xenografts and 2D and 3D cocultures of NHFs and PDAC cells revealed that older NHFs stimulate proliferation of and confer resistance to radiation therapy of PDAC. MS-based metabolite analysis indicated that older NHFs have significantly increased arachidonic acid 12-lipoxygenase (ALOX12) expression and elevated levels of its mitogenic metabolite, 12-(*S*)-hydroxy-5,8,10,14-eicosatetraenoic acid (12-(*S*)-HETE) compared with their younger counterparts. In cocultures with older rather than with younger NHFs, PDAC cells exhibited increases in mitogen-activated protein kinase signaling and cellular metabolism, as well as a lower oxidation state that correlated with their enhanced proliferation and resistance to radiation therapy. Expression of ALOX12 was found to be significantly lower in PDAC cell lines and tumor biopsies, suggesting that PDAC cells rely on a stromal supply of mitogens for their proliferative needs. Pharmacological (hydroxytyrosol) and molecular (siRNA) interventions of ALOX12 in older NHFs suppressed their ability to stimulate proliferation of PDAC cells. We conclude that chronological aging of NHFs contributes to PDAC progression and that ALOX12 and 12-(*S*)-HETE may be potential stromal targets for interventions that seek to halt progression and improve therapy outcomes.

The incidence of pancreatic cancer increases with age; median age at diagnosis is 71 years old and the median age at death is 73 years old, suggesting that chronological aging is a significant risk factor for pancreatic cancer. Pancreatic ductal adenocarcinoma (PDAC)[2] ranks fourth among cancer-related deaths in the United States: it has a very high incidence of recurrence and a dismal 5-year survival rate of less than 8% (1, 2) (RRID: SCR_006902). Recent evidence suggests that the tumor microenvironment significantly influences progression and therapy of cancer (4–10). PDAC tissue is stroma-rich, dense, and fibrous (11, 12). The stroma of PDAC includes fibroblasts, myofibroblasts, stellate cells, immune cells, and endothelial cells (8). Fibroblasts are the major noncancerous cell type contributing to the cellularity of the stroma that include synthesis and remodeling of the extracellular matrix as well as the production of secretory and nonsecretory factors that influence cancer cell proliferation and progression to end stage disease. Because age is a significant risk factor for PDAC, it is important to know whether the age of the stroma influences progression of PDAC and the mechanisms involved in this process.

Chronologically aged normal human fibroblasts (NHF) (quiescent fibroblasts aged *in vitro*) are known to stimulate proliferation of human breast cancer cells (13). C-C motif chemokine ligand 5, which is overexpressed in chronologically aged NHFs, has been shown to activate the extracellular signal-regulated kinase (ERK)1/2-cyclin D1 pathway in breast cancer cells resulting in the stimulation of their proliferation (13). Although quiescent cells are not actively proliferating, they are metabolically active. Significant changes in metabolism have been observed during chronological aging of NHFs (14). Metabolism

This work was supported by two separate Pilot Project Awards from the University of Iowa HCCC and the Center on Aging (to P. C. G. and E. H. S.), the Kansas City University of Medicine and Biosciences Intramural Grant Discovery Program (to E. H. S.), and National Institutes of Health Grants P01CA217797 (to J. J. C.) and T32 CA148062 (to M. S. A.). The authors declare that they have no conflicts of interest with the contents of this article. The content is solely the responsibility of the authors and does not necessarily represent the official views of the National Institutes of Health.

This article contains Fig. S1, Table S1, and Supporting Methods.

[1] To whom correspondence should be addressed: Free Radical & Radiation Biology Division, Dept. of Radiation Oncology, The University of Iowa, Iowa City, IA 52242. Tel.: 319-384-4666; Fax: 319-335-8039; E-mail: prabhat-goswami@uiowa.edu.

[2] The abbreviations used are: PDAC, human pancreatic ductal adenocarcinoma; 12-(*S*)-HETE, 12-(*S*)-hydroxy-5,8,10,14-eicosatetraenoic acid; AA, arachidonic acid; ALOX, arachidonic acid lipoxygenase; NHF, normal human fibroblasts; PTGS-1 and -2, prostaglandin-endoperoxide synthase; ERK, extracellular signal-regulated kinase; PPP, pentose phosphate pathway; DHE, dihydroethidium; Gy, gray; qPCR, quantitative PCR; MAPK, mitogen-activated protein kinase.

of quiescent cultures of NHFs from younger (newborn to 1 year old) donors were found to be more glycolytic compared with NHFs from older (29–70 years old) donors that exhibited significant increases in mitochondrial respiration. These previously published results led us to the novel hypothesis that an age-related change in metabolism of the stroma contributes to the progression of epithelial cancer.

An increase in mitochondrial respiration and decrease in glycolysis in older NHFs suggest that changes in lipid metabolism during aging can influence stroma-directed progression of PDAC. Lipid-signaling pathways are known to regulate proliferation and therapy of cancer cells (15–19). Eicosanoids are a family of lipid mediators derived from the metabolism of arachidonic acid (AA). AA is converted to eicosanoids by cyclooxygenase and arachidonic acid lipoxygenase (ALOX) enzymes. Based on their regiospecificity, human ALOXs are grouped into three major groups: ALOX5, ALOX12, and ALOX15. The enzymatic products of ALOXs are hydroperoxyeicosatetraenoic acids, which are converted to hydroxyeicosatetraenoic acids (HETEs) (20, 21). 12-(*S*)-HETE is a mitogenic metabolite of ALOX12. The signaling and mitogenic properties of 12-(*S*)-HETE can be mediated by its binding to the membrane-bound G protein–coupled receptors; GPR31 is a high-affinity receptor for 12-(*S*)-HETE (22). Eicosanoids, which include prostaglandins and leukotrienes, are well-known for their inflammation and immune properties (23). These lipid mediators are also known to have mitogenic properties (23, 24).

Results from this study show that the chronological aging of the stroma regulates progression and radiation therapy resistance of PDAC. ALOX12 and 12-(*S*)-HETE are potential targets of the aging stroma that can be considered to halt progression and improve therapy of PDAC.

Results

NHFs from older healthy donors stimulate proliferation of PDAC cells

To determine whether chronological aging of NHFs regulates progression of PDAC, we used a novel murine xenograft approach where co-cultures of CellTracker Green-labeled NHFs and luciferase expressing MIA PaCa-2 cells (10:1) embedded in injectable tissue-like 3D gel matrix were injected into the flank of 30-day-old athymic female nude mice (*Foxn*1^{nu}). Bioluminescence imaging system (Xenogen IVIS-200) was used to measure proliferation. Results clearly show the presence of CellTracker Green-labeled NHFs and luciferase expressing MIA PaCa-2 cells in the xenograft (Fig. 1*A*). The presence of NHFs in tumors was also evident from the confocal microscopy analysis of excised tumor tissues (Fig. 1*B*) and flow cytometry analysis of cell suspensions prepared from resected tumors (Fig. 1*C*). Measurements of tumor volume showed 2× tumor volume in xenografts carrying co-cultures of MIA PaCa-2 cells and NHFs from a 61-year-old healthy donor compared with tumor volume in co-cultures of MIA PaCa-2 cells and NHFs from a 3-day-old healthy donor. Increases in tumor volume correlated with a shorter median survival of a 34-day-old compared with a median survival of 44 days of mice carrying xenograft of MIA PaCa-2 cells and NHFs from a 3-day-old donor (Fig. 1, *D* and *E*). An age-related stimulation of proliferation of MIA PaCa-2 cells in co-cultures of older compared with young NHFs was also observed in an orthotopic xenograft approach (Fig. S1). Overall, these results support our novel hypothesis that chronological aging of the stroma regulates progression of PDAC.

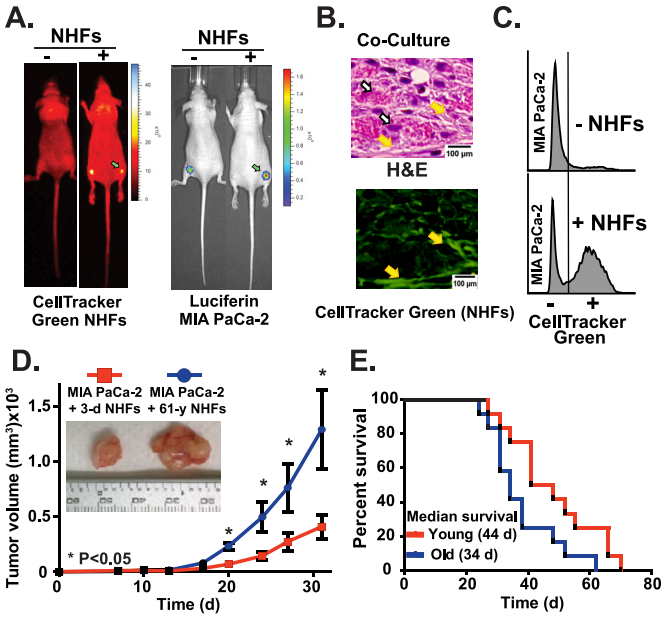

Figure 1. Older NHFs stimulate proliferation of MIA PaCa-2 human PDAC cells *in vivo*. *A,* 3D gel matrix-embedded co-cultures of CellTracker Green-labeled NHFs and luciferase expressing MIA PaCa-2-Luc cells were injected into the flank of mice, and imaged when palpable tumors were detected. $n = 2$. *B,* H&E and fluorescent microscopy detection of NHFs (*yellow arrows*) and MIA PaCa-2 cells (*white arrows*). *C,* flow cytometry analysis of cell suspensions prepared from excised tumors: CellTracker Green-positive (NHFs) and negative (MIA PaCa-2-Luc) cells. *D,* tumor volume of co-cultures of NHFs and MIA PaCa-2 cells; *inset* shows representative resected tumors. *Asterisks* represent significance; mean ± S.D.; $n = 10$, $p < 0.05$. *E,* Kaplan-Meyer plot of survival; $n = 10$, $p < 0.05$.

Results from these *in vivo* experiments were also recapitulated in 3D and 2D co-cultures *in vitro*. A mixture of luciferase expressing MIA PaCa-2-Luc cells and quiescent cultures of NHFs (10:1) were embedded into the Cell Mate 3D matrix and co-cultured for different days. Photon counts showed approximately a 4-fold increase of MIA PaCa-2-Luc cells co-cultured with quiescent cultures of NHFs from a 61-year-old healthy donor (Fig. 2, *A* and *B*). The doubling time of MIA PaCa-2-Luc cells co-cultured with NHFs from a 61-year-old donor was ~20 h compared with a doubling time of 60 h for MIA PaCa-2-Luc cells co-cultured with NHFs from a 3-day-old donor (Fig. 2*B*). Similar to the co-existence of MIA PaCa-2-Luc cells and NHFs in tumor xenograft *in vivo* (Fig. 1, *A–C*), results from H&E staining and fluorescence microscopy also showed the presence of NHFs (*black arrow*) and MIA PaCa-2 cells (*white arrow*) in the 3D co-cultures (Fig. 2*B*, *inset*), suggesting that the 3D co-culture method can partially mimic the tumor microenvironment *in vitro*.

To determine whether the age of the stroma can also influence therapy of PDAC, 3D co-cultures of quiescent NHFs and PDAC-Luc cells were irradiated with a shortened clinical protocol, 2 Gy × 5 days. Results showed that the rate of proliferation of MIA PaCa-2-Luc cells is consistently higher in irradi-

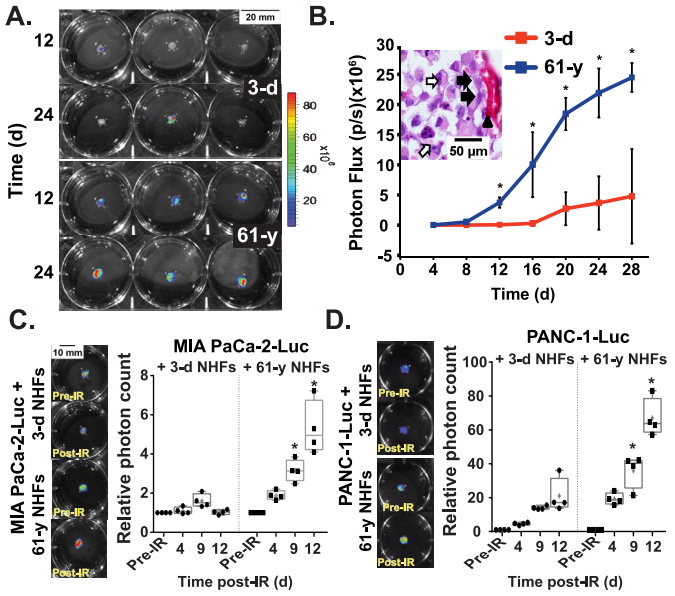

Figure 2. Chronological aging of NHFs influences progression and therapy of human PDAC cells in 3D co-cultures. *A,* pseudo-color scale of photons s^{-1} emitted from individual 3D spheres of co-cultures of NHFs and MIA PaCa-2-luc cells. *B,* photon counts of MIA PaCa-2-luc cells in co-cultures; *inset* shows H&E staining of sliced spheres: fibroblasts (*black arrows*), cancer cells (*white arrows*). Photon counts of (*C*) MIA PaCa-2-Luc and (*D*) PANC-1-Luc cells in 3D co-cultures of NHFs post-radiation (2 Gy × 5 days). *Asterisks* represent significance; $n = 3$, $p < 0.05$.

ated co-cultures of NHFs from a 61-year-old donor at 4–12 days post-irradiation compared with co-cultures with NHFs from a 3-day-old healthy donor (Fig. 2*C*). Comparable results were also obtained from co-cultures using a separate PDAC cell line, PANC-1-Luc (Fig. 2*D*). These results support the hypothesis that chronological aging of the stroma significantly affects proliferation and radiation therapy of PDAC cells.

The age difference between the two NHFs (61 years old *versus* 3 days old) and our earlier observation of chronological aging of NHFs stimulating proliferation of breast cancer cells (13, 25–27) suggest that the chronological aging of the stroma can significantly influence progression of PDAC. To further investigate this hypothesis, quiescent cultures of NHFs from a 3-day-old donor were aged *in vitro* for 7 (early) and 60 (late) days. CellTracker Green-labeled MIA PaCa-2 cells were then added on top of the unlabeled quiescent lawns of NHFs. 2D co-cultures of MIA PaCa-2 cells and NHFs were continued *in vitro* for an additional 2–6 days. Microscopy imaging and flow cytometry methods (13) were used to measure proliferation of MIA PaCa-2 cells in co-cultures of NHFs. Microscopy evaluation of the density of MIA PaCa-2 cells showed a significant increase in proliferation of MIA PaCa-2 cells co-cultured with late-NHFs (3-fold increase at 6 days of co-culture) (Fig. 3*A*). The doubling time for MIA PaCa-2 cells co-cultured with quiescent cultures of late-NHFs was calculated to be 23 h compared with a doubling time of 33 h for MIA PaCa-2 cells co-cultured with early-NHFs (Fig. 3*B*). These results were further confirmed by flow cytometry analysis of the percentage of MIA PaCa-2 cells in co-cultures of early- and late-NHFs; there was more than 60% increase in the number of MIA PaCa-2 cells co-cultured with late-NHFs compared with early-NHFs (Fig. 3*C*). These results clearly show that quiescent cultures of NHFs that are chronologically aged *in vitro* also promote proliferation of PDAC cells. To rigorously test this novel observation of chronological aging affecting progression of PDAC, additional 2D co-culture experiments were performed using NHFs from donors of different ages. Results showed a significant increase in the percentage of MIA PaCa-2 cells from 7% in co-cultures of quiescent cultures of NHFs from a 3-day-old donor to 18 and 30% in co-cultures with NHFs from 12- and 61-year-old healthy donors, respectively (Fig. 3, *D* and *E*). Comparable results were also observed in co-cultures of NHFs and PANC-1 and BxPC-3 PDAC cell lines (Fig. 3*E*). Additionally, a small but statistically significant increase in proliferation of nonmalignant H6c7 pancreatic ductal epithelial cells was also observed in co-cultures of NHFs from a 61-year-old donor (Fig. 3*E*). These results showed that the chronological aging of NHFs promotes proliferation of both malignant and nonmalignant pancreatic ductal epithelial cells, but the growth stimulatory effects are significantly higher in malignant compared with nonmalignant cells.

Results from the 3D co-culture experiments demonstrating radiation resistance of PDAC cells in co-cultures of old compared with young NHFs (Fig. 2*D*) were also recapitulated in experiments using 2D co-cultures. CellTracker Green-labeled MIA PaCa-2 cells were layered upon confluent cultures of NHFs from 3-day-old and 12- and 61-year-old healthy donors. Co-cultures at 5 days post-plating were irradiated with 0, 2, and 4 Gy ionizing radiation and continued in culture. The percentage of CellTracker Green-labeled MIA PaCa-2 cells in control and irradiated co-cultures was analyzed by flow cytometry. Results showed a significant increase in the percentage of MIA PaCa-2 cells in un-irradiated control co-cultures of 12- and 61-year-old compared with 3-day-old NHFs; approximately, 15 and 30% MIA PaCa-2 cells in co-cultures of 12- and 61-year-old NHFs compared with 5% MIA PaCa-2 cells in co-cultures of 3-day-old NHFs (Fig. 4*A*). Co-cultures irradiated with 4 Gy radiation showed a significant decrease in the percentage of MIA PaCa-2 cells in all co-cultures compared with their respective un-irradiated controls (Fig. 4*A*). However, the decrease in the percentage of MIA PaCa-2 cells in irradiated co-cultures of 61-year-old NHFs was significantly less than co-cultures with 12-year-old and 3-day-old NHFs (Fig. 4*A*), further suggesting that aging NHFs confer radiation resistance of MIA PaCa-2 cells. Indeed, flow cytometry analysis of radiation-induced toxicity of MIA PaCa-2 cells in co-cultures of NHFs showed maximal cell death in co-cultures of 3-day compared with 12- and 61-year-old NHFs (Fig. 4*B*). Overall, these results showed that quiescent cultures of NHFs from donors of older compared with younger healthy individuals stimulate proliferation and induce radiation therapy resistance of PDAC cells (Figs. 1–4).

ALOX12 and 12-(S)-HETE mediate fibroblasts' chronological aging-induced stimulation of proliferation of PDAC cells

We previously reported significant increases in mitochondrial respiration rates and decreases in glycolytic flux in NHFs from 29–70–year-old healthy donors (14), demonstrating that changes in cellular metabolism occur during chronological aging of NHFs. To determine whether specific metabolic processes are altered during chronological aging, metabolomics profiling was performed (University of Iowa Metabolomics

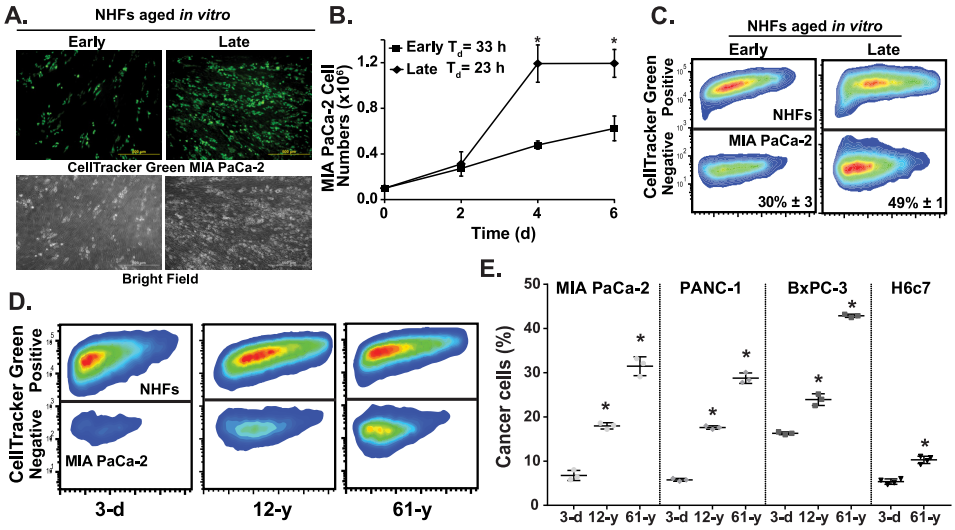

Figure 3. Older NHFs stimulate proliferation of PDAC cells in 2D co-cultures. *A,* microscopy pictures of 5-day co-cultures of NHFs and CellTracker Green-labeled MIA PaCa-2 cells. *B,* growth of CellTracker Green-labeled MIA PaCa-2 cells in co-cultures of NHFs. *C,* flow cytometry analysis of MIA PaCa-2 cells in co-cultures of NHFs. *D,* representative flow cytometry histograms showing distributions of NHFs and MIA PaCa-2 cells in co-cultures. *E,* percentage of PDAC cells in co-cultures of NHFs from donors of different ages. *Asterisks* represent significance; $n = 3$, $p < 0.05$.

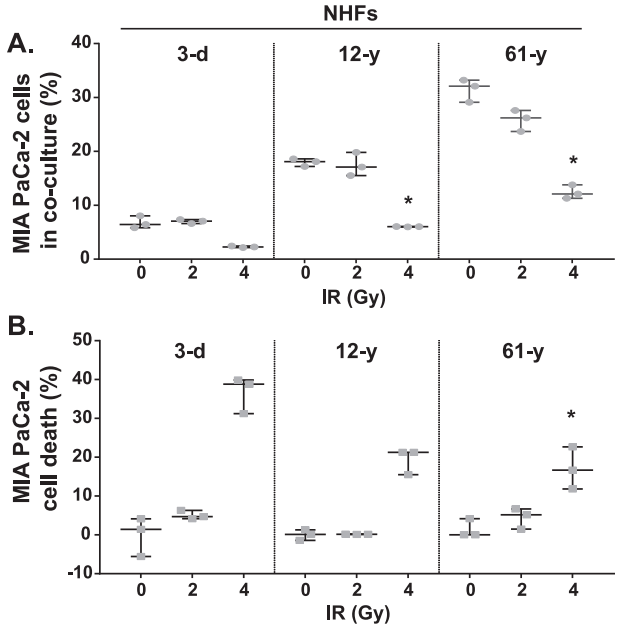

Figure 4. Resistance of MIA PaCa-2 cells to radiation treatments in 2D co-cultures of old compared with young NHFs. CellTracker Green-labeled MIA PaCa-2 cells were layered over confluent cultures of NHFs from 3-day- and 12- and 61-year-old healthy donors. At the end of 5 days of co-cultures, cells were irradiated with 0, 2, and 4 Gy of ionizing radiation. Flow cytometry was used to identify and quantitate CellTracker Green-positive (MIA PaCa-2) and negative (NHFs) cells. Proliferation of MIA PaCa-2 cells was assessed from the decreases in CellTracker Green fluorescence per cell. *A,* percent of MIA PaCa-2 cells in control and irradiated co-cultures of NHFs; *B,* percent of MIA PaCa-2 cell death in control and irradiated co-cultures; $n = 3$, $p < 0.05$.

Core Facility). A semi-targeted high-resolution GC-MS protocol was used to quantitatively measure metabolites of the TCA cycle, glycolytic intermediates, amino acids, sugars, and fatty acids. Results showed significant increases in fatty acids levels of NHFs from older healthy donors, mostly in the 18–22 carbon fatty acids (Fig. 5*A*). Among this group of fatty acids, levels of AA (C20:4) showed an increase of ~2-fold. AA is converted to eicosanoids by cyclooxygenase and ALOX enzymes. Initially, a RT-qPCR assay was performed to determine whether an age-related increase in AA metabolism could be due to an increase in the expression of prostaglandin-endoperoxide synthase (PTGS-1 and -2) and arachidonic acid lipoxygenase (ALOX5, -12, and -15) enzymes. Results showed no significant difference in the expression of PTGS-1 and -2, and ALOX5 and ALOX15 between the 61-year- and 3-day-old NHFs. However, a significant difference in the expression of ALOX12 was observed in the 61-year-old NHFs: a ~6-fold increase in mRNA levels (Fig. 5*B*) and 2-fold increase in protein levels (Fig. 5*B*, *inset*). This intriguing observation of an age-related increase in ALOX12 expression was further evident from a corresponding increase in its secreted metabolite, 12-(*S*)-HETE. Levels of 12-(*S*)-HETE were significantly lower (<10 fg cell^{-1}) in NHFs from a 3-day- and 5-month-old healthy donor compared with 10–35 fg cell^{-1} in NHFs from the 58–70–year-old group (Fig. 5*C*). To further verify that the increases in 12-(*S*)-HETE levels are true representation of the chronological aging process, NHFs from a 3-day healthy donor were aged in quiescence for 7 (early) and 60 (late) days. Consistent with the results of 12-(*S*)-HETE levels in NHFs from donors of different ages (Fig. 5*C*), early-NHFs showed significantly lower levels of 12-(*S*)-HETE (<10 fg cell^{-1}) compared with more than 20 fg cell^{-1} in late-NHFs (Fig. 5*D*). Overall, these results showed significant increases in the expression of ALOX12 and its metabolite, 12-(*S*)-HETE during the chronological aging of NHFs.

Considering the mitogenic property of 12-(*S*)-HETE (28, 29), we hypothesize that 12-(*S*)-HETE secreted from the aging stroma stimulates proliferation of PDAC cells via a paracrine signaling pathway. To test this novel hypothesis, we first measured mRNA levels of ALOX12 in established PDAC cell lines (MIA PaCa-2 and PANC-1), recently generated patient-derived PDAC cell lines (339 and 403), and a transformed but nonmalignant (H6c7) human pancreatic epithelial cell line. Expression of ALOX12 in all four PDAC cell lines was significantly lower compared with its expression in the nonmalignant cell line, H6c7 (Fig. 5, *E* and *F*). Next, we examined whether the receptor

A.

Lipid metabolites, 61-y *vs.* 3-d NHFs	
Metabolite	**Fold Change**
Arachidic acid/Eicosanoic acid (C20)	2.0
Behenic acid/Docosanoic acid (C22)	1.8
Citraconate/Citraconic acid	1.8
Heneicosanoic acid (C21)	2.3
Linoleic acid	2.0
Oleic acid	1.9
Palmitic acid	2.2
Stearic acid	2.5

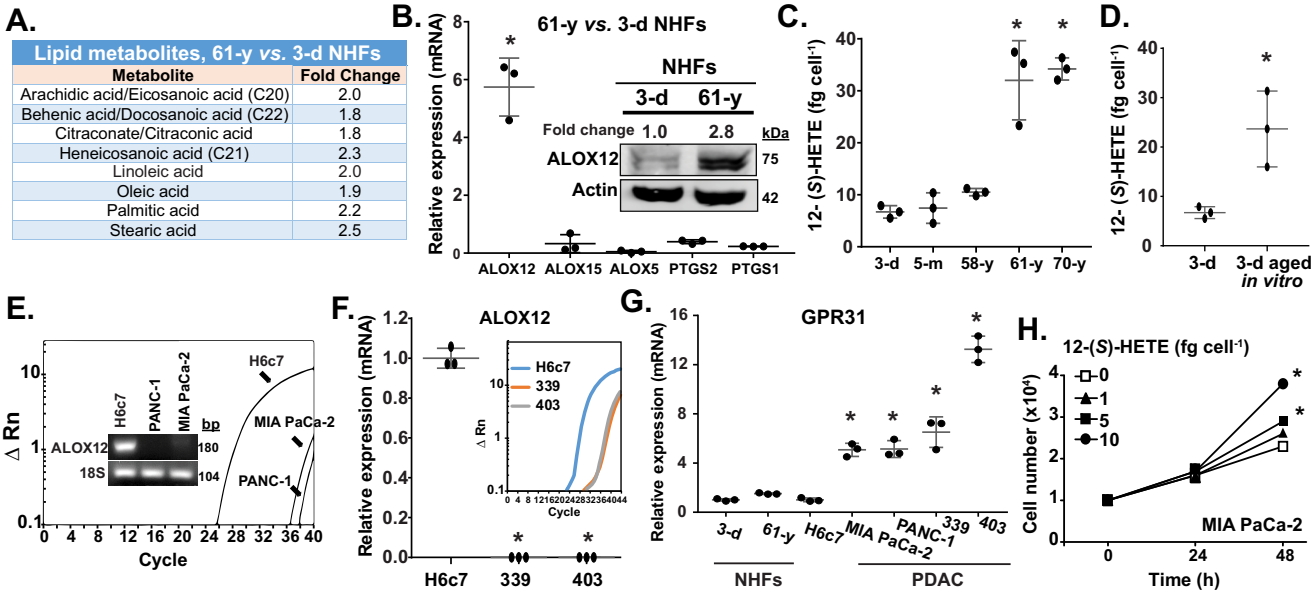

Figure 5. An age-related increase in ALOX12 expression and 12-(*S*)-HETE is associated with old NHFs-induced stimulation of PDAC cells. *A,* mass spectrometry analysis of lipid metabolites in conditioned media of 3-day-old and 61-year-old NHFs. Fold-change was calculated relative to metabolites in 3-day-old NHFs. *B,* RT-qPCR analysis of arachidonic acid-metabolizing enzymes; *inset* shows immunoblot analysis of ALOX12. An ELISA-based assay was used to quantitatively measure 12-(*S*)-HETE levels in conditioned media collected from: *C,* quiescent cultures of NHFs from donors of different ages and *D,* 3-day-old NHFs that were aged in culture. RT-qPCR analysis: ALOX12 expression in: *E,* PDAC cell lines obtained from ATCC and *F,* newly generated PDAC cell lines from surgically resected and de-identified human PDAC tissues. *G,* RT-qPCR analysis of GPR31 mRNA expression. *H,* proliferation of MIA PaCa-2 cells in the presence of exogenously added 12-(*S*)-HETE. *Asterisks* represent significance; $n = 3$, $p < 0.05$.

for 12-(*S*)-HETE, GPR31, is differentially expressed in normal compared with PDAC cells. Expression of GPR31 was found to be significantly lower in NHFs and H6c7 cells compared with a 6–14–fold increase in the PDAC cell lines (Fig. 5*G*). These results suggest that whereas 12-(*S*)-HETE secreted from NHFs may not affect their own proliferation because of significantly lower expression of GPR31 and quiescent growth state, they can have a paracrine effect on neighboring PDAC cells that have significantly higher expression of GPR31. This premise is supported from results presented in Fig. 5*H*. A dose-dependent increase in the number of MIA PaCa-2 cells was observed when different concentrations (1–10 fg cell^{-1}) of 12-(*S*)-HETE were added to the medium and cells were cultured for 24–48 h (Fig. 5*H*). Overall, these results suggest that 12-(*S*)-HETE secreted from the aging stroma initiates a paracrine mitogenic effect that results in enhanced proliferation of PDAC cells.

Increases in MAPK signaling pathways and metabolism combined with a lower oxidation status of PDAC cells in co-cultures of old NHFs

We have previously shown that quiescent cultures of 3-day NHFs aged *in vitro* induced ERK1/2-cyclin D1 proliferative pathway in human breast cancer cells resulting in their enhanced proliferation (13). To determine whether older NHFs-induced proliferation of PDAC cells (Figs. 1–4) is associated with the induction of MAPK pathways, MIA PaCa-2 cells were first separated from co-cultures of NHFs by flow cytometry-based cell sorting. RayBiotech MAPK pathway phosphorylation arrays were used to measure the phosphorylation status of pro-proliferative signaling proteins. Although phosphorylation (active form) of most of the proliferative-signaling proteins increased in MIA PaCa-2 cells co-cultured with 61-year-old

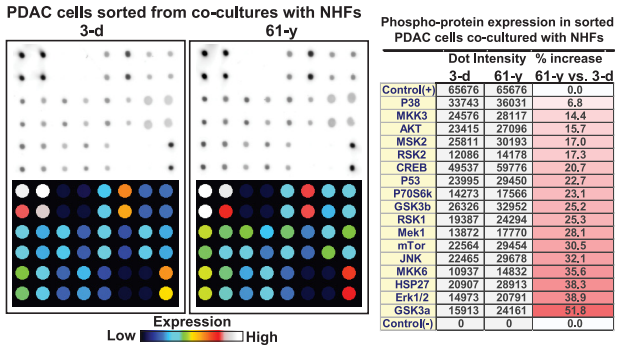

Phospho-protein expression in sorted PDAC cells co-cultured with NHFs

	Dot Intensity		% increase
	3-d	61-y	61-y vs. 3-d
Control(+)	65676	65676	0.0
P38	33743	36031	6.8
MKK3	24576	28117	14.4
AKT	23415	27096	15.7
MSK2	25811	30193	17.0
RSK2	12086	14178	17.3
CREB	49537	59776	20.7
P53	23995	29450	22.7
P70S6k	14273	17566	23.1
GSK3b	26326	32952	25.2
RSK1	19387	24294	25.3
Mek1	13872	17770	28.1
mTor	22564	29454	30.5
JNK	22465	29678	32.1
MKK6	10937	14832	35.6
HSP27	20907	28913	38.3
Erk1/2	14973	20791	38.9
GSK3a	15913	24161	51.8
Control(-)	0	0	0.0

Figure 6. Metabolic and proliferative signaling pathways are enhanced in PDAC cells co-cultured with older NHFs. RayBiotech MAPK Pathway Phosphorylation Arrays were used to analyze the phosphorylation status of signaling proteins of MIA PaCa-2 cells sorted from co-cultures of NHFs. Visualization and quantification of results were performed using a Typhoon 7000 phosphorimager (GE Healthcare) and NIH ImageJ software. *Left panels*, images of the original blots and heat maps; *right panel*, quantitative results. Percent increase in phosphoproteins of 61-year-old NHFs was calculated relative to 3-day-old NHFs.

compared with 3-day-young NHFs, increases in the ERK1/2, and mTOR signaling pathways were more pronounced (Fig. 6). These results suggest that increases in the ERK1/2 and mTOR signaling pathways can mediate enhanced proliferation of PDAC cells in co-cultures of old compared with young NHFs.

Increases in glucose and mitochondrial metabolism during progression from G_0-G_1 to S-G_2-M phases suggest that cellular metabolism is intimately linked to cellular proliferation (30). To determine whether chronological aging of NHFs alters the metabolism of PDAC cells that results in their enhanced proliferation, flow cytometry-based cell sorting was used first to separate MIA PaCa-2 cells from 2D co-cultures of quiescent NHFs and then metabolites of MIA PaCa-2 cells were analyzed using a Thermo Q Exactive GC-MS Orbitrap instrument (UIOWA

A. Metabolites upregulated in PDAC cells sorted from co-culture with NHFs (61-y vs. 3-d)

Glycolysis	
Metabolite	Fold Change
Glucose	8
Fructose 6 - phosphate	23
Lactate	4
Pyruvate	2
PPP	
Metabolite	Fold Change
Ribose 5 - phosphate	25
Sedoheptulose	3
Sedoheptulose 7 - phosphate	56

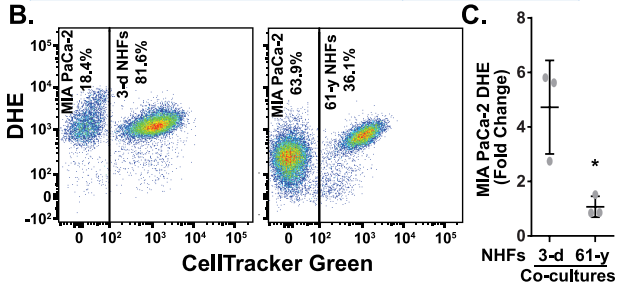

Figure 7. Increases in metabolism combined with a lower oxidation status of PDAC cells co-cultured with old compared with young NHFs. *A,* flow cytometry sorted MIA PaCa-2 cells from co-cultures of CellTracker Green-labeled NHFs were used for analysis of metabolites (UIOWA HCCC Metabolomics Core). Results were normalized to cell mass and fold-change calculated relative to metabolites of MIA PaCa-2 cells co-cultured with 3-day-old NHFs. *B* and *C,* flow cytometry analysis of DHE-oxidation in co-cultures of CellTracker Green-labeled NHFs and MIA PaCa-2 cells. *Asterisk* represents significance compared with 3-day-old NHFs; $n = 3$, $p < 0.05$.

HCCC Metabolomics Core). Results showed significant increases in the metabolites of the glycolytic (glucose, fructose 6-phosphate, lactate, and pyruvate) and pentose phosphate pathway (PPP: ribose 5-phosphate and sedoheptulose 7-phosphate) in MIA PaCa-2 cells co-cultured with NHFs from a 61-year-old compared with a 3-day-old healthy donor (Fig. 7*A*). These results suggest that increases in cellular metabolism of PDAC cells can mediate their enhanced proliferation in co-cultures of old compared with young NHFs.

To determine whether older NHFs-induced increases in glycolysis and PPP of MIA PaCa-2 cells also impact their redox status, co-cultures were incubated with dihydroethidium (DHE). DHE oxidation was analyzed by flow cytometry (30). Consistent with results presented in Fig. 3, the percentage of the MIA PaCa-2 cells was higher in co-cultures of quiescent NHFs from the 61-year-old compared with 3-day-old healthy donor (Fig. 7*B*). It is interesting to note that the DHE oxidation was significantly lower in MIA PaCa-2 cells co-cultured with NHFs from the 61-year-old compared with 3-day-old healthy donor (Fig. 7*C*). These results suggest that older NHFs facilitate a reducing environment of MIA PaCa-2 cells by rewiring their metabolism to glycolysis and PPP. Overall, these results (Figs. 6 and 7) suggest that older NHFs promote proliferation of PDAC cells by enhancing the MAPK signaling pathways and cellular metabolism that favor a reducing environment supporting proliferation of PDAC cells.

Pharmacological and molecular interventions of ALOX12 and 12-(S)-HETE in older NHFs suppress their abilities to stimulate proliferation of PDAC cells

There is growing interest in the use of polyphenols to minimize age-related health issues (31–33). Hydroxytyrosol, a major polyphenol of olives, has been shown to inhibit activity of ALOX12 (34–36). To determine whether hydroxytyrosol treatment affects 12-(*S*)-HETE levels in NHFs, quiescent cultures of NHFs from a 61-year-old donor were cultured in medium containing 100 μM hydroxytyrosol. An ELISA-based assay was used to measure 12-(*S*)-HETE in conditioned medium. Results showed more than 50% decrease in 12-(*S*)-HETE levels in hydroxytyrosol-treated NHFs compared with untreated controls (Fig. 8*A*). Consistent with earlier results (Figs. 1–4), quiescent cultures from a 61-year-old healthy donor stimulated proliferation of MIA PaCa-2 cells as evident from the significant increase in the percentage of MIA PaCa-2 cells in co-cultures of NHFs (Fig. 8*B*, *upper panels*). However, such an increase in proliferation of MIA PaCa-2 cells is significantly suppressed in co-cultures of hydroxytyrosol-treated quiescent cultures of NHFs (Fig. 8*B*, *lower panels*). Comparable results were also obtained when experiments were repeated using 3-day-old NHFs that were chronologically aged *in vitro*. Plating efficiency of MIA PaCa-2 cells cultured in conditioned medium collected from control treatment increased to 40% in conditioned medium collected from late-NHFs compared with 20% in medium collected from early-NHFs (Fig. 8*C*). However, plating efficiency of MIA PaCa-2 cells cultured in conditioned medium collected from hydroxytyrosol-treated early- and late-NHFs is significantly suppressed (Fig. 8*C*). These results suggest a role of 12-(*S*)-HETE regulating proliferation of MIA PaCa-2 cells in co-cultures of NHFs.

The causality of ALOX12 regulating old NHF-induced stimulation of proliferation of PDAC cells was also investigated using a siRNA molecular approach. Treatment with siALOX12 decreased its expression by ~50% in NHFs from a 61-year-old donor (Fig. 8*D*, *upper panel*). Flow cytometry analysis of 2D co-cultures that were performed using CellTracker Green-labeled NHFs and MIA PaCa-2 cells showed a significant decrease in the percentage of MIA PaCa-2 cells (~35%) co-cultured with siALOX12-treated NHFs compared with 50% in co-cultures with control and scramble-siRNA treated NHFs (Fig. 8*D*, *lower panel*). Overall, results from the pharmacological and molecular approaches clearly showed a mechanistic role of ALOX12 and its metabolite 12-(*S*)-HETE regulating old NHFs induced stimulation of proliferation of PDAC cells.

Clinical correlation of ALOX12 and 12-(S)-HETE with PDAC progression and therapy

The clinical significance of our basic science research was determined by measuring ALOX12 and 12-(*S*)-HETE in PDAC patients' samples. Initially, the Oncomine database was used to analyze microarray transcriptome profiling data that were collected by Buchholz *et al.* (37) from pancreatic intraepithelial neoplastic lesions, pancreas intraepithelial neoplasia, pancreas ductal adenocarcinoma, and normal pancreas duct. Bioinformatics evaluation of these data set revealed a significant down-regulation of the expression of ALOX12 in pancreas carcinoma compared with pancreas cancer precursor and normal pancreas duct (Fig. 9*A*). Using de-identified surgical samples of PDAC and plasma samples (provided by Dr. J. Cullen; samples were collected from a Phase I trial, NCT number 01852890 for PDAC therapy) (38), we examined protein expression of

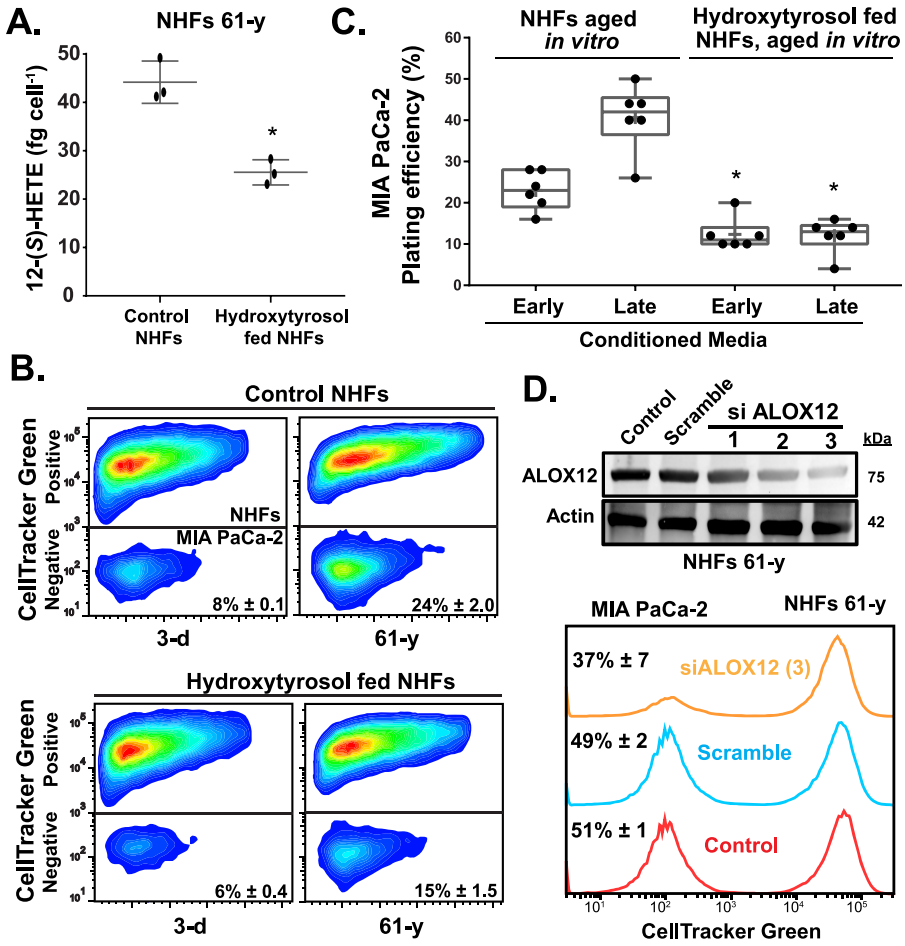

Figure 8. Hydroxytyrosol and siALOX12 treatments suppress older NHFs induced stimulation of PDAC proliferation. *A,* 12-(*S*)-HETE levels in conditioned media from 10-day quiescent cultures of control and 100 μM hydroxytyrosol-treated NHFs. *B,* flow cytometry analysis of the percentage of MIA PaCa-2 cells in co-cultures of CellTracker Green-labeled control and hydroxytyrosol-treated NHFs. *C,* plating efficiency of MIA PaCa-2 cells cultured in conditioned media from control and hydroxytyrosol-treated NHFs. *Asterisks* represent statistical significance; $n = 3$, $p < 0.05$. *D, upper panel*: immunoblot analysis of ALOX12 protein levels in control, scrambled siRNA, and siALOX12 treated 61-year-old NHFs. *Lower panel*: flow cytometry analysis of the percentage of MIA PaCa-2 cells in co-cultures of NHFs.

ALOX12 in biopsies and 12-(*S*)-HETE levels in plasma samples. Results showed that the protein levels of ALOX12 were significantly lower in PDAC cells compared with nearby nonmalignant cells (Fig. 9*B*), which is also consistent with the Oncomine data (Fig. 9*A*). A higher level of 12-(*S*)-HETE was observed in all patients' plasma samples post-therapy compared with pre-therapy (Fig. 9*C*). Within the post-therapy samples, a correlation was observed between 12-(*S*)-HETE levels and incidence of recurrence and metastasis: higher levels of 12-(*S*)-HETE correlating with higher incidence of recurrence and metastasis in PDAC patients (Fig. 9, *D* and *E*). These results attest to the clinical significance of our basic science research. In summary, results from this study showed the significance of the chronological aging of normal human fibroblasts in pancreatic cancer and identified ALOX12 and 12-(*S*)-HETE as novel molecular regulators of stromal aging-induced progression and therapy outcomes of PDAC (Fig. 9*F*).

Discussion

Like all cancers, the incidence of PDAC increases exponentially with age (3). Although a majority of PDAC research focuses on understanding the cellular and molecular control of the epithelial cancer cells, we investigated whether the chronological aging of normal cells regulates progression and therapy outcomes of PDAC, and the mechanisms involved in this process. Our results showed fibroblasts from older healthy donors stimulate proliferation and confer resistance to radiation therapy of human PDAC cells. Results from pharmacological and molecular approaches identified ALOX12 and its metabolite 12-(*S*)-HETE contributing to older fibroblasts' induced stimulation of proliferation and radiation resistance of PDAC cells.

Replicative and chronological lifespan are two of the most widely studied modes of cellular aging (39–41). Chronological lifespan represents the duration of quiescence during which normal cells retain their capacity to re-enter the proliferative cycle (25, 26). We previously reported that the chronological aging of fibroblasts is independent of mitotic division and telomerase activity (25). Our results also showed quiescent cultures of NHFs from a 3-day-old healthy donor that were chronologically aged in culture to stimulate proliferation of human breast cancer cells (13). The present study was designed to investigate whether naturally aged NHFs influence progression and therapy of PDAC cells. Results from *in vivo* murine xenograft of co-cultures of NHFs and human MIA PaCa-2 cells

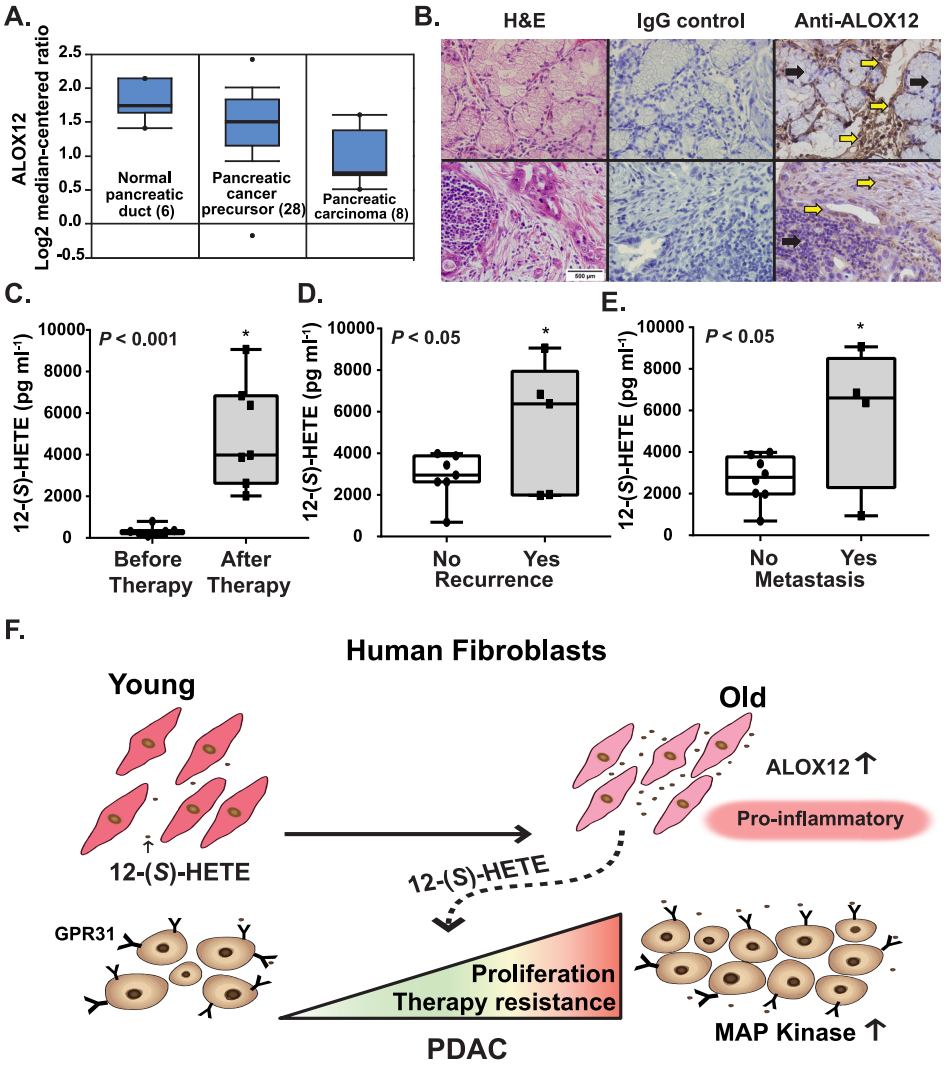

Figure 9. ALOX12 and 12-(*S*)-HETE are potential stromal-aging biomarkers for PDAC progression and therapy response. *A,* Oncomine data analysis of ALOX12 expression in pancreas cancer (37). *B,* immunohistochemistry analysis of ALOX12 in paraffin-embedded and de-identified resected PDAC tissues: *black arrows*, PDAC cells; *yellow arrows*, nonmalignant stromal cells. *C,* 12-(*S*)-HETE levels in de-identified plasma samples from 14 PDAC patients. Results were evaluated for incidence of (*D*) recurrence and (*E*) metastasis. *Asterisks* represent significance, $p < 0.05$, measured by paired *t* test. *F,* an illustration showing increases in ALOX12 expression and 12-(*S*)-HETE levels during chronological aging of NHFs promoting PDAC progression by enhancing MAPK signaling pathways and metabolism. It is hypothesized that increases in metabolism combined with a reducing status confer resistance of PDAC cells to therapy in an aging-stromal environment.

showed a higher tumor volume in co-cultures of older NHFs and MIA PaCa-2 cells, which was also associated with a lower median survival (Fig. 1, *D* and *E*). Comparable results were also obtained from 3D and 2D co-cultures of MIA PaCa-2 cells and quiescent cultures of NHFs from donors of different ages (Figs. 2, *A* and *B,* and 3). Similar results were also obtained from 2D co-culture experiments that were performed using PANC-1 and BxPC-3 PDAC cells (Fig. 3*E*). A small but statistically significant increase in the proliferation of H6c7 (transformed but nonmalignant) human pancreatic epithelial cells was also observed (Fig. 3*E*). NHFs' age-induced proliferation of PDAC cells appear to be independent of the k-*ras* genotype status of PDAC cells. Older NHFs stimulated proliferation of both WT (BxPC-3) and mutant (MIA PaCa-2 and PANC-1) k-*ras* cells (Fig. 2*A*). Additional results showed that the older NHFs confer radiation resistance of MIA PaCa-2 and PANC-1 cells (Figs. 2, *C* and *D,* and 4). Overall, our earlier results of chronologically aged *in vitro* cultures of NHFs stimulating proliferation of breast cancer cells (13) and results (Figs. 1–4) from this study clearly show that the chronological aging of NHFs is a critical factor in progression and therapy outcomes of PDAC.

In 1966 Stoker *et al.* (42) first reported quiescent cultures of rodent fibroblasts inhibiting proliferation of polyoma-transformed rodent fibroblasts. Flaberg *et al.* (43) used a high-throughput live-cell imaging method to study the effects of 107 human fibroblasts on proliferation of human prostate cancer cells *in vitro*. Although all primary cultures of fibroblasts inhibited growth of the prostate cancer cells, pediatric fibroblasts showed a higher inhibitory effect compared with adult fibroblasts. Although the authors did not address the age effect of these fibroblasts, their results did invoke the hypothesis that the age of the stroma (fibroblasts) is a significant factor in epithelial cancer progression. Indeed, laser capture microdissection and gene expression analysis of human breast cancer tissues did

show a distinct stromal-aging footprint in older compared with younger patients (44). Consistent with these literature reports, our results also showed an age-effect of NHFs stimulating proliferation of PDAC cells (Figs. 1–4). Based on single-cell transcriptomic analysis, recent studies report the presence of at least three different types of fibroblasts in the PDAC stroma: fibroblasts exhibiting myofibroblastic features (αSMA^{high}) that surround the malignant PDAC and fibroblasts exhibiting inflammatory (cytokine and chemokine positive) and antigen-presenting properties that reside distally from the PDAC cells (45–47). Based on our observation of higher ALOX12 expression and higher levels of its metabolite 12-(*S*)-HETE (inflammatory signature) in older NHFs (Fig. 5), we speculate that the distally localized fibroblasts with the inflammatory phenotype represent the aging stroma and they contribute to the stromal age-related progression of PDAC.

We previously reported a shift in cellular metabolism from glycolysis in young to mitochondrial respiration in older NHFs (14). Decreases in extracellular acidification rates and increases in oxygen consumption rates during chronological lifespan of NHFs (14) suggest that metabolic pathways other than glycolysis are involved with the age-related increases in respiration of NHFs. Mitochondrial respiration also receives substrates from lipid metabolism, suggesting that the age-related increases in respiration of NHFs could be due to a change in their lipid metabolism. Indeed, results from MS analysis of metabolites showed significant increases in free fatty acid levels of older compared with young NHFs (Fig. 5*A*). An age-related increase in AA metabolism of NHFs was also evident from the corresponding increases in the expression of ALOX12 and its mitogenic metabolite, 12-(*S*)-HETE (Fig. 5, *B–D*). It is interesting to note that the expression of ALOX12 was significantly lower in established (Fig. 5*E*) and newly generated (Fig. 5*F*) patient-derived PDAC cell lines, whereas the expression of GPR31 (receptor for 12-(*S*)-HETE) was significantly higher in PDAC cells compared with NHFs and H6c7 nonmalignant pancreatic epithelial cells (Fig. 5, *E–G*). These results support the hypothesis that a paracrine signaling from older NHFs provides a mitogenic environment for PDAC cells. Although 12-(*S*)-HETE secreted from older NHFs may not stimulate their own proliferation due to a lower level of expression of GPR31, it is anticipated to provide mitogenic stimuli to PDAC cells due to their higher level of expression of GPR31. Indeed, exogenously added 12-(*S*)-HETE dose-dependently enhanced proliferation of MIA PaCa-2 cells (Fig. 5*H*).

Consistent with our earlier results of chronologically aged 3-day NHFs enhancing the ERK1/2 pathway that resulted in significant increases in proliferation of breast cancer cells (13), results from the MAPK arrays also showed significant increases in the ERK1/2 and mTOR pathways in MIA PaCa-2 cells that were associated with their enhanced proliferation in co-cultures of old compared with young NHFs (Fig. 6). As anticipated, increases in the ERK1/2 and mTOR pathways were also associated with increases in cellular metabolism (glycolysis and PPP) of MIA PaCa-2 cells in co-cultures of old compared with young NHFs (Fig. 7*A*). Whereas the nonoxidative pathway of the PPP is involved in nucleotide biosynthesis (ribose 5-phosphate), the oxidative pathway of the PPP promotes a reducing environment (NADPH, GSH). Indeed, old NHFs-induced increases in the PPP of MIA PaCa-2 cells were associated with a lower oxidation status compared with the oxidation status of MIA PaCa-2 cells co-cultured with young NHFs (Fig. 7, *B* and *C*). A lower oxidation status (reducing environment) is anticipated to favor proliferation and therapy resistance of MIA PaCa-2 cells in co-cultures of old compared with young NHFs. This premise is consistent with results presented in Figs. 1–7.

Results from pharmacological and molecular approaches clearly showed a role of ALOX12 and 12-(*S*)-HETE contributing to old NHF-induced proliferation of PDAC cells (Fig. 8). Because expression of ALOXs is down-regulated in human bladder, breast, lung, colon, and prostate cancer cells (3, 48, 49), our results also suggest that ALOXs and their metabolites HEPTEs and HETEs provide a stromal aging-derived mitogenic axis that promotes cancer progression and confer resistance to therapy. The clinical significance of our basic science research is evident from our observation of a significant decrease in ALOX12 expression in PDAC cells compared with their neighboring nonmalignant cells as well as plasma levels of 12-(*S*)-HETE correlating with therapy outcomes, recurrence, and metastasis (Fig. 9, *A–E*).

In summary, our results showed that the chronological aging of NHFs is a critical regulator of progression and therapy outcomes of PDAC. Intervention of the aging stroma by targeting ALOX12 expression (Fig. 9*F*) can be a novel approach to prevent progression and improve therapy of PDAC.

Experimental procedures

Additional details of the experimental procedures are included under the "Supporting Materials".

Cell culture and reagents

All cell cultures (Table S1) were performed using Dulbecco's modified Eagle's medium (Gibco) supplemented with 10% fetal bovine serum and antibiotics in humidified incubators with ambient oxygen concentration. Measurements in NHFs were performed using individual and primary cultures from donors of different ages; samples were not pooled. Microscopy and flow cytometry assays were used to visualize and quantitate the percentage of NHFs and PDAC cells in co-cultures. Luciferase expressing PDAC cells and Cell Mate 3D Gel matrix (BRTI Life Sciences) were used for the 3D co-culture experiments. Photon counts (Xenogen IVIS 200 system) were used to measure proliferation of luciferase expressing PDAC cells in 3D co-cultures. Hydroxytyrosol was purchased from the Cayman Chemical. A shortened clinical radiation therapy protocol (2 Gy × 5 days; dose rate 0.6 Gy min^{-1}) was used to irradiate co-cultures.

Murine tumor xenograft

All animal experiments were reviewed and approved by the Animal Care and Use Committee of The University of Iowa; approval number 1311211-001. Cell Mate 3D Gel matrix-embedded co-cultures of CellTracker Green-labeled NHFs and luciferase expressing MIA PaCa-2 cells (10:1) were injected into the flank of 5-week-old female athymic mice, and imaged when palpable tumors were detected. Microscopy and flow cytometry methods were used to identify NHFs and MIA PaCa-2 cells

in the excised xenograft. In a separate set of experiments, tumor volume of xenograft carrying co-cultures of NHFs and MIA PaCa-2 cells was measured using a digital caliper.

Analysis of metabolites

A ThermoQ Exactive Mass Spectrometer (The UIOWA Metabolomics Core Facility) was used to analyze metabolites in cells and conditioned media. Xcailbur Tracefinder 4.1 software was used for data analysis.

RT-qPCR assay

Total cellular RNA was extracted using TRIzol reagent (Invitrogen) and quantified using a NanoDrop-1000 Spectrophotometer (Thermo Fisher Scientific). One microgram of total RNA was reverse-transcribed using High Capacity cDNA Reverse Transcription Kit (Applied Biosystems). cDNAs were used for Real-Time PCR amplification using the Power SYBR Green Master Mix (Applied Biosystems) and StepOne Plus™ System (Applied Biosystems) following our published method (30).

siRNA knockdown

Quiescent cultures of NHFs were transfected with scrambled (SR30004) and siALOX12 (SR300166; OriGene) using Lipofectamine 2000 (Invitrogen) following the manufacturers protocol. Immunoblotting assay was used to measure the efficiency of siRNA knockdown of ALOX12 expression at 48–96 h post-transfection.

Immunoblotting assay

Cell pellets were pulse-sonicated (Vibra-Cell Cup Horn; Sonics and Materials Inc.) and equal amounts of protein lysates were separated on SDS-PAGE followed by semi-dry electroblotting to nitrocellulose membrane (Bio-Rad Labs). Membranes were incubated with antibodies to human ALOX12 (Milipore-Sigma) and β-actin (Abcam). Pierce™ ECL 2 Western blotting Substrate (Thermo Scientific) and Typhoon FLA 7000 (GE Healthcare) were used to visualize immune-reactive polypeptides.

Immunohistochemistry assay

De-identified PDAC tissues and plasma samples were obtained from Dr. Cullen's recently completed phase I trial (NCT number 01852890) designed to examine the safety of pharmacological ascorbate with gemcitabine for the treatment of pancreatic cancer. Paraffin-embedded and de-identified surgical tissue sections were dewaxed and processed for analysis of ALOX12 expression using primary ALOX12 antibody (Millipore-Sigma), horseradish peroxidase-linked secondary antibody, and 3,3′-diaminobenzidine as the chromogen. Slides were counterstained with Harris hematoxylin and images were recorded using microscopy.

ELISA

Enzo life Sciences ELISA kit (ADI-900-050) was used to quantify 12-(*S*)-HETE levels in plasma samples of 14 PDAC patients.

Statistical methods

SPSS software was used for all statistical analysis. For experiments with three or more continuous variables, statistical analysis was performed using the one- or two-way analysis of variance with Tukey's honestly significant difference. Homogeneity of variance is assumed with 95% confidence interval level. Results from at least $n \geq 3$ with $p < 0.05$ are considered significant. Group survival was summarized with Kaplan-Meier plots and compared with log-rank and Gehan-Breslow-Wilcoxon tests.

Data availability

All the data described are contained within the manuscript and associated supporting information.

Author contributions—E. H. S. and P. C. G. conceptualization; E. H. S., J. M. S., A. L. K., W. X., J. D., M. S. A., B. R. O., J. J. C., and P. C. G. data curation; E. H. S., J. M. S., A. L. K., J. D., M. S. A., B. R. O., J. J. C., and P. C. G. formal analysis; E. H. S., J. J. C., and P. C. G. supervision; E. H. S., J. M. S., J. J. C., and P. C. G. funding acquisition; E. H. S., J. M. S., and P. C. G. investigation; E. H. S. and J. M. S. methodology; E. H. S. and J. M. S. writing-original draft; P. C. G. resources; P. C. G. validation; P. C. G. project administration; P. C. G. writing-review and editing.

Acknowledgments—We thank Dr. Eric Taylor, Director of the University of Iowa Metabolomics Core Facility and his team Dr. Lynn Teesh, Dr. Adam Rauckhorst, and Alvin Pewa for their help with MS, and Gareth Smith for editorial assistance. Flow Cytometry, Central Microscopy, and Radiation and Free Radical Research Core facilities were supported by National Institute of Health NCI P30CA086862.

References

1. Hidalgo, M. (2010) Pancreatic cancer. *N. Engl. J. Med.* **362,** 1605–1617 CrossRef Medline
2. Yip, D., Karapetis, C., Strickland, A., Steer, C. B., and Goldstein, D. (2006) Chemotherapy and radiotherapy for inoperable advanced pancreatic cancer. *Cochrane Database Syst. Rev.* **19,** CD002093 Medline
3. Tang, D. G., Bhatia, B., Tang, S., and Schneider-Broussard, R. (2007) 15-Lipoxygenase 2 (15-LOX2) is a functional tumor suppressor that regulates human prostate epithelial cell differentiation, senescence, and growth (size). *Prostaglandins Other Lipid Mediat.* **82,** 135–146 CrossRef Medline
4. Fang, H., and Declerck, Y. A. (2013) Targeting the tumor microenvironment: from understanding pathways to effective clinical trials. *Cancer Res.* **73,** 4965–4977 CrossRef Medline
5. Kadaba, R., Birke, H., Wang, J., Hooper, S., Andl, C. D., Di Maggio, F., Soylu, E., Ghallab, M., Bor, D., Froeling, F. E., Bhattacharya, S., Rustgi, A. K., Sahai, E., Chelala, C., Sasieni, P., and Kocher, H. M. (2013) Imbalance of desmoplastic stromal cell numbers drives aggressive cancer processes. *J. Pathol.* **230,** 107–117 CrossRef Medline
6. Kalluri, R., and Zeisberg, M. (2006) Fibroblasts in cancer. *Nat. Rev. Cancer* **6,** 392–401 CrossRef Medline
7. Krtolica, A., and Campisi, J. (2003) Integrating epithelial cancer, aging stroma and cellular senescence. *Adv. Gerontol.* **11,** 109–116 Medline
8. Lunardi, S., Muschel, R. J., and Brunner, T. B. (2014) The stromal compartments in pancreatic cancer: are there any therapeutic targets? *Cancer Lett.* **343,** 147–155 CrossRef Medline
9. Waghray, M., Yalamanchili, M., di Magliano, M. P., and Simeone, D. M. (2013) Deciphering the role of stroma in pancreatic cancer. *Curr. Opin. Gastroenterol.* **29,** 537–543 CrossRef Medline
10. Yachida, S., and Iacobuzio-Donahue, C. A. (2013) Evolution and dynamics of pancreatic cancer progression. *Oncogene* **32,** 5253–5260 CrossRef Medline

11. Hartel, M., Di Mola, F. F., Gardini, A., Zimmermann, A., Di Sebastiano, P., Guweidhi, A., Innocenti, P., Giese, T., Giese, N., Büchler, M. W., and Friess, H. (2004) Desmoplastic reaction influences pancreatic cancer growth behavior. *World J. Surg.* **28,** 818–825 CrossRef Medline
12. Hwang, R. F., Moore, T., Arumugam, T., Ramachandran, V., Amos, K. D., Rivera, A., Ji, B., Evans, D. B., and Logsdon, C. D. (2008) Cancer-associated stromal fibroblasts promote pancreatic tumor progression. *Cancer Res.* **68,** 918–926 CrossRef Medline
13. Sarsour, E. H., Goswami, M., Kalen, A. L., Lafin, J. T., and Goswami, P. C. (2014) Hydroxytyrosol inhibits chemokine C-C motif ligand 5 mediated aged quiescent fibroblast-induced stimulation of breast cancer cell proliferation. *Age* **36,** 9645 CrossRef Medline
14. Son, J. M., Sarsour, E. H., Kakkerla Balaraju, A., Fussell, J., Kalen, A. L., Wagner, B. A., Buettner, G. R., and Goswami, P. C. (2017) Mitofusin 1 and optic atrophy 1 shift metabolism to mitochondrial respiration during aging. *Aging Cell* **16,** 1136–1145 CrossRef Medline
15. Sunami, Y., Rebelo, A., and Kleeff, J. (2017) Lipid metabolism and lipid droplets in pancreatic cancer and stellate cells. *Cancers (Basel)* **10,** piiE3 Medline
16. Stoykova, G. E., and Schlaepfer, I. R. (2019) Lipid metabolism and endocrine resistance in prostate cancer, and new opportunities for therapy. *Int. J. Mol. Sci.* **20,** e2626 Medline
17. Long, J., Zhang, C. J., Zhu, N., Du, K., Yin, Y. F., Tan, X., Liao, D. F., and Qin, L. (2018) Lipid metabolism and carcinogenesis, cancer development. *Am. J. Cancer Res.* **8,** 778–791 Medline
18. Corbet, C., and Feron, O. (2017) Emerging roles of lipid metabolism in cancer progression. *Curr. Opin. Clin. Nutr. Metab. Care* **20,** 254–260 CrossRef Medline
19. Kanikarla-Marie, P., Kopetz, S., Hawk, E. T., Millward, S. W., Sood, A. K., Gresele, P., Overman, M., Honn, K., and Menter, D. G. (2018) Bioactive lipid metabolism in platelet "first responder" and cancer biology. *Cancer Metastasis Rev.* **37,** 439–454 CrossRef Medline
20. Gotoh, Y., Noda, T., Iwakiri, R., Fujimoto, K., Rhoads, C. A., and Aw, T. Y. (2002) Lipid peroxide-induced redox imbalance differentially mediates CaCo-2 cell proliferation and growth arrest. *Cell Prolif.* **35,** 221–235 CrossRef Medline
21. Wang, H. P., Schafer, F. Q., Goswami, P. C., Oberley, L. W., and Buettner, G. R. (2003) Phospholipid hydroperoxide glutathione peroxidase induces a delay in G1 of the cell cycle. *Free Radic. Res.* **37,** 621–630 CrossRef Medline
22. Guo, Y., Zhang, W., Giroux, C., Cai, Y., Ekambaram, P., Dilly, A. K., Hsu, A., Zhou, S., Maddipati, K. R., Liu, J., Joshi, S., Tucker, S. C., Lee, M. J., and Honn, K. V. (2011) Identification of the orphan G protein-coupled receptor GPR31 as a receptor for 12-(*S*)-hydroxyeicosatetraenoic acid. *J. Biol. Chem.* **286,** 33832–33840 CrossRef Medline
23. Wang, D., and Dubois, R. N. (2010) Eicosanoids and cancer. *Nat. Rev. Cancer* **10,** 181–193 CrossRef Medline
24. Wang, D., and Dubois, R. N. (2006) Prostaglandins and cancer. *Gut* **55,** 115–122 CrossRef Medline
25. Sarsour, E. H., Agarwal, M., Pandita, T. K., Oberley, L. W., and Goswami, P. C. (2005) Manganese superoxide dismutase protects the proliferative capacity of confluent normal human fibroblasts. *J. Biol. Chem.* **280,** 18033–18041 CrossRef Medline
26. Sarsour, E. H., Venkataraman, S., Kalen, A. L., Oberley, L. W., and Goswami, P. C. (2008) Manganese superoxide dismutase activity regulates transitions between quiescent and proliferative growth. *Aging Cell* **7,** 405–417 CrossRef Medline
27. Sarsour, E. H., Goswami, M., Kalen, A. L., and Goswami, P. C. (2010) MnSOD activity protects mitochondrial morphology of quiescent fibroblasts from age associated abnormalities. *Mitochondrion* **10,** 342–349 CrossRef Medline
28. Ding, X. Z., Tong, W. G., and Adrian, T. E. (2001) 12-lipoxygenase metabolite 12(*S*)-HETE stimulates human pancreatic cancer cell proliferation via protein tyrosine phosphorylation and ERK activation. *Int. J. Cancer* **94,** 630–636 CrossRef Medline
29. Setty, B. N., Graeber, J. E., and Stuart, M. J. (1987) The mitogenic effect of 15- and 12-hydroxyeicosatetraenoic acid on endothelial cells may be mediated via diacylglycerol kinase inhibition. *J. Biol. Chem.* **262,** 17613–17622 Medline
30. Sarsour, E. H., Kalen, A. L., Xiao, Z., Veenstra, T. D., Chaudhuri, L., Venkataraman, S., Reigan, P., Buettner, G. R., and Goswami, P. C. (2012) Manganese superoxide dismutase regulates a metabolic switch during the mammalian cell cycle. *Cancer Res.* **72,** 3807–3816 CrossRef Medline
31. Santos, C. N., Gomes, A., Oudot, C., Dias-Pedroso, D., Rodriguez-Mateos, A., Vieira, H. L. A., and Brenner, C. (2018) Pure polyphenols applications for cardiac health and disease. *Curr. Pharm. Des.* **24,** 2137–2156 CrossRef Medline
32. Silva, LBAR., Pinheiro-Castro, N., Novaes, G. M., Pascoal, G. F. L., and Ong, T. P. (2019) Bioactive food compounds, epigenetics and chronic disease prevention: focus on early-life interventions with polyphenols. *Food Res. Int.* **125,** 108646 CrossRef Medline
33. Zhang, P. Y. (2015) Polyphenols in health and disease. *Cell Biochem. Biophys.* **73,** 649–664 CrossRef Medline
34. Petroni, A., Blasevich, M., Salami, M., Papini, N., Montedoro, G. F., and Galli, C. (1995) Inhibition of platelet aggregation and eicosanoid production by phenolic components of olive oil. *Thromb. Res.* **78,** 151–160 CrossRef Medline
35. Petroni, A., Blasevich, M., Papini, N., Salami, M., Sala, A., and Galli, C. (1997) Inhibition of leukocyte leukotriene B4 production by an olive oil-derived phenol identified by mass-spectrometry. *Thromb. Res.* **87,** 315–322 CrossRef Medline
36. Souza, P. A. L., Marcadenti, A., and Portal, V. L. (2017) Effects of olive oil phenolic compounds on inflammation in the prevention and treatment of coronary artery disease. *Nutrients* **9,** e1087 Medline
37. Buchholz, M., Braun, M., Heidenblut, A., Kestler, H. A., Kloppel, G., Schmiegel, W., Hahn, S. A., Lüttges, J., and Gress, T. M. (2005) Transcriptome analysis of microdissected pancreatic intraepithelial neoplastic lesions. *Oncogene* **24,** 6626–6636 CrossRef Medline
38. Du, J., Cieslak, J. A. 3rd, Welsh, J. L., Sibenaller, Z. A., Allen, B. G., Wagner, B. A., Kalen, A. L., Doskey, C. M., Strother, R. K., Button, A. M., Mott, S. L., Smith, B., Tsai, S., Mezhir, J., Goswami, P. C., Spitz, D. R., Buettner, G. R., and Cullen, J. J. (2015) Pharmacological ascorbate radiosensitizes pancreatic cancer. *Cancer Res.* **75,** 3314–3326 CrossRef Medline
39. Maskell, D. L., Kennedy, A. I., Hodgson, J. A., and Smart, K. A. (2003) Chronological and replicative lifespan of polyploid *Saccharomyces cerevisiae* (syn. *S. pastorianus*). *FEMS Yeast Res.* **3,** 201–209 CrossRef Medline
40. Polymenis, M., and Kennedy, B. K. (2012) Chronological and replicative lifespan in yeast: do they meet in the middle? *Cell Cycle* **11,** 3531–3532 CrossRef Medline
41. Postnikoff, S. D., and Harkness, T. A. (2014) Replicative and chronological life-span assays. *Methods Mol. Biol.* **1163,** 223–227 CrossRef Medline
42. Stoker, M. G., Shearer, M., and O'Neill, C. (1966) Growth inhibition of polyoma-transformed cells by contact with static normal fibroblasts. *J. Cell Sci.* **1,** 297–310 Medline
43. Flaberg, E., Markasz, L., Petranyi, G., Stuber, G., Dicso, F., Alchihabi, N., Olàh, E., Csìzy, I., Józsa, T., Andrén, O., Johansson, J. E., Andersson, S. O., Klein, G., and Szekely, L. (2011) High-throughput live-cell imaging reveals differential inhibition of tumor cell proliferation by human fibroblasts. *Int. J. Cancer* **128,** 2793–2802 CrossRef Medline
44. Brouwers, B., Fumagalli, D., Brohee, S., Hatse, S., Govaere, O., Floris, G., Van den Eynde, K., Bareche, Y., Schöffski, P., Smeets, A., Neven, P., Lambrechts, D., Sotiriou, C., and Wildiers, H. (2017) The footprint of the ageing stroma in older patients with breast cancer. *Breast Cancer Res.* **19,** 78 CrossRef Medline
45. Biffi, G., Oni, T. E., Spielman, B., Hao, Y., Elyada, E., Park, Y., Preall, J., and Tuveson, D. A. (2019) IL1-induced JAK/STAT signaling is antagonized by TGFβ to shape CAF heterogeneity in pancreatic ductal adenocarcinoma. *Cancer Discov.* **9,** 282–301 CrossRef Medline
46. Elyada, E., Bolisetty, M., Laise, P., Flynn, W. F., Courtois, E. T., Burkhart, R. A., Teinor, J. A., Belleau, P., Biffi, G., Lucito, M. S., Sivajothi, S., Armstrong, T. D., Engle, D. D., Yu, K. H., Hao, Y., *et al.* (2019) Cross-species single-cell analysis of pancreatic ductal adenocarcinoma reveals antigen-presenting cancer-associated fibroblasts. *Cancer Discov.* **9,** 1102–1123 CrossRef Medline

47. Öhlund, D., Handly-Santana, A., Biffi, G., Elyada, E., Almeida, A. S., Ponz-Sarvise, M., Corbo, V., Oni, T. E., Hearn, S. A., Lee, E. J., Chio, I. I., Hwang, C. I., Tiriac, H., Baker, L. A., Engle, D. D., *et al*. (2017) Distinct populations of inflammatory fibroblasts and myofibroblasts in pancreatic cancer. *J. Exp. Med.* **214,** 579–596 CrossRef Medline
48. Shureiqi, I., Wojno, K. J., Poore, J. A., Reddy, R. G., Moussalli, M. J., Spindler, S. A., Greenson, J. K., Normolle, D., Hasan, A. A., Lawrence, T. S., and Brenner, D. E. (1999) Decreased 13-S-hydroxyoctadecadienoic acid levels and 15-lipoxygenase-1 expression in human colon cancers. *Carcinogenesis* **20,** 1985–1995 CrossRef Medline
49. Subbarayan, V., Xu, X. C., Kim, J., Yang, P., Hoque, A., Sabichi, A. L., Llansa, N., Mendoza, G., Logothetis, C. J., Newman, R. A., Lippman, S. M., and Menter, D. G. (2005) Inverse relationship between 15-lipoxygenase-2 and PPAR-γ gene expression in normal epithelia compared with tumor epithelia. *Neoplasia* **7,** 280–293 CrossRef Medline